MR imaging of cardiac wall-motion at 1.5T and 7T: SNR and CNR comparison

S. Maderwald[1,2], K. Nassenstein[1,2], S. Orzada[1,2], L. C. Schäfer[1,2], M. Oehmigen[1], A. K. Bitz[1,2], O. Kraff[1,2], I. Brote[1,2], S. C. Ladd[1,2], M. E. Ladd[1,2], and H. H. Quick[1,3]

[1]Erwin L. Hahn Institute for Magnetic Resonance Imaging, Essen, Germany, [2]Department of Diagnostic and Interventional Radiology and Neuroradiology, University Hospital Essen, Essen, Germany, [3]Institute of Medical Physics, Friedrich-Alexander-University Erlangen-Nürnberg, Erlangen, Germany

Introduction: In vivo cardiac MRI at ultra high field (7T) in humans has been demonstrated (1, 2), revealing several challenges to be overcome to compete with cardiac MRI at clinical field strengths (up to 3T). In this study some of the major challenges of 7T cardiac MRI have been addressed and a dedicated custom-built 8-ch Tx/Rx RF coil has been used to compare 1.5T with 7T short-axis cine images with regards to SNR and CNR. The purpose of this study thus was to show and to quantify potential benefits or limitations of 7T clinical human in vivo MRI for cardiac function.

Materials and Methods: The 1.5T examinations were performed on a Magnetom Avanto (Siemens Healthcare Sector, Erlangen, Germany) equipped with a gradient system capable of 45 mT/m maximum amplitude and a slew rate of 220 mT/m/ms. For signal reception, the vendor provided spine matrix RF coil (6 RF coil elements) and one body matrix coil (6 RF coil elements) were used in the triple mode. The 7T examinations were performed on a whole-body MRI system (Magnetom 7T, Siemens) equipped with an identical gradient system. A custom-built 8-channel Tx/Rx RF coil (3) with 4 elements integrated into the patient table and 4 flexible elements positioned on top of the human chest was used for 7T cardiac imaging. Each coil channel was driven by an individual 1 kW power amplifier (Dressler LPPA 13080W, Germany), and RF shimming (4) was performed by an 8-channel vector modulator (5) with SAR monitoring by an in-house developed supervision system (6). Simulations based on a male member (70 kg, 1.74 m) of the virtual family (7) were used to calculate amplitudes and phases of each of the 8 RF channels to obtain homogenization of the transmit B_1 field over the region of the heart. While the amplitudes were kept constant for all channels, the phases of coil channels 1 to 8 were 9°, 278°, 0°, 187°, 252°, 216°, 263°, 42°, respectively. For cardiac imaging, five healthy volunteers (3 male, 2 female; mean height 1.8 m ± 0.1 m and mean weight 73.4kg ± 8.7 kg) were placed in both scanners head-first supine with the chest at the isocenter of the magnet. At 1.5T, the ECG trigger was used for all examinations. At 7T, however, ECG triggering was often limited due to the challenges associated with the increased magnetohydrodynamic (MHD) potential of flowing blood in strong magnetic fields, resulting in inaccurate trigger signals. In these cases, peripheral pulse triggering was used. The imaging protocol encompassed cardiac function along the short axis. At 1.5T the standard clinically used Cine SSFP sequence (TR/TE 39.7/1.12 ms; FOV 340 x 289 mm^2; matrix 192 x 163; slice 6 mm; BW 930 Hz/pixel; flip 76°, 20 phases per RR-interval, TA 0:09 min) was used, whereas at 7T images were acquired with a Cine FLASH (spoiled gradient echo) sequence (TR/TE 29/3.5 ms; FOV 340 x 306 mm^2; matrix 240 x 216; slice 5 mm; BW 992 Hz/pixel; flip 40°, 20 phases per RR-interval, TA 0:29 min). The Cine SSFP sequence at 7T was not used due to known problems and artifacts associated with high field SSFP imaging (2). In order to use a regions-of-interest (ROI) based SNR and CNR measuring algorithm, all short-axis views were scanned without parallel imaging techniques. For SNR and CNR calculation, signal intensity (SI) measurements were carried out in locally adapted ROIs (i.e. in the left ventricular cavity and in each segment (8) of the left ventricular (LV) myocardium. Noise was defined as standard deviation from a signal intensity measurement in a circular ROI outside the body (air in the field-of-view, anterior to the chest wall). SNR and CNR were calculated as follows: SNR = SI / image noise, $CNR_{blood\text{-}myocardium} = (SI_{blood} - SI_{myocardium}) /$ image noise. In total, 160 myocardium ROIs (16 segments, 2 slices, 5 subjects), 60 blood ROIs (6 regions, 2 slices, 5 subjects) and 30 noise ROIs (3 regions, 2 slices, 5 subjects) were evaluated for each field strength.

Results: All 5 subjects tolerated both cardiac examinations well and could be successfully examined. The positioning on the table including the anterior coil placement was considered comfortable at both field strengths. Although the peripheral pulse trigger occasionally led to mild motion blurring, it seems to be more suitable for 7T at this point as compared to ECG triggering which often failed due to physiologic changes in the ECG waveform associated with the strong magnetic field. About 80% of all sequences at 7T were gated with the pulse trigger. The coil at 7T, when driven in the simulated shim mode, qualitatively provided relatively homogeneous B_1 signal over the heart volume. In a few images, mild destructive interference associated with signal voids could be seen in some regions. Nevertheless, the Cine FLASH sequence provided good image quality with good signal homogeneity over almost the entire cardiac volume. The 7T Cine FLASH (Fig. 1A) in comparison to the 1.5T Cine SSFP (Fig. 1B) showed much higher SNR and CNR values (Table 1).

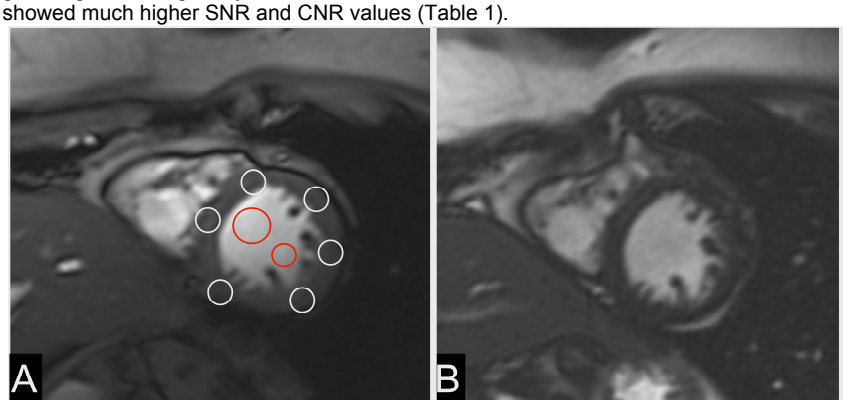

Figure 1: Short-axis views of a Cine FLASH at 7T (A) with the ROIs (myocardium (white) and blood (red)) and of a Cine SSFP at 1.5T (B). Note that FLASH at 7T and SSFP at 1.5T provide comparable image contrast behavior.

	7T	1.5T
Mean SI myocardium	51.5 ± 19.5	82.0 ± 49.4
Mean SI blood	210.3 ± 59.3	437.5 ± 72.2
Mean Noise	0.9 ± 0.2	5.0 ± 1.0
Mean SNR	59.6 ± 20.6	15.9 ± 5.5
Mean CNR	205.5 ± 82.4	74.5 ± 24.2

Table 1: Signal, noise, and contrast values measured as Mean ± SD of 5 volunteers at 7T and 1.5T. A t-test provides statistically significant p values ($p < 0.0001$) for all criteria.

Discussion: While at 1.5T B_1 inhomogeneities were not present, new RF transmit/receive strategies were needed at 7T to overcome the known limitations associated with 7T body imaging. The heart shim worked well at 7T in all 5 volunteers. For perfectly timed and triggered cardiac images, ECG triggering seems mandatory, as peripheral pulse gating, as mostly used at 7T in this study, in part was associated with imprecise triggering leading to mild motion artifacts in the Cine acquisitions. Nevertheless, the Cine FLASH sequences subjectively provided excellent image quality, myocardium-to-blood contrast, and spatial resolution for the evaluation of cardiac function e.g. in the short-axis orientation. The quantitatively measured image quality (SNR and CNR) at 7T outperforms the results at 1.5T. One explanation for the small noise values measured at 7T in comparison to 1.5T may result from the differences in the RF coil design and RF setup. At 7T, a transmit/receive RF coil was used which needs no detuning circuit and hence no PIN diodes in the receive path of the coil. The obvious limitation of this comparison study is the use of different sequence types (SSFP vs. FLASH) with different voxel volumes (19.44 ml^3 vs. 9.8 ml^3) and a varying TA (9 s vs. 29 s) between 1.5T and 7T, rendering a side-by-side comparison of a single sequence type with identical imaging parameters at both magnetic field strengths open. For this comparison study, it was thus intended to image with the sequence type that performs best for each field strength (i.e. SSFP at 1.5T and FLASH at 7T). Therefore, from this comparison study the conclusion can be drawn that with the demonstrated increases in SNR and CNR, 7T cardiac function MRI with FLASH has the potential to outperform cardiac function MRI with SSFP at 1.5T, but further evaluation with clinical pathologies will be required.

References:
[1] Snyder et al., MRM 61:517-524 (2009); [2] Maderwald et al. Proc. Intl. Soc. MRM (2009) (Abstract 821); [3] Orzada et al., Proc. Intl. Soc. MRM (2009) (Abstract 3010); [4] Bitz et al., Proc. Intl. Soc. MRM (2009) (Abstract 4767); [5] Yazdanbakhsh et al., Proc. Intl. Soc. MRM (2009) (Abstract 4768); [6] Brote et al., Proc. Intl. Soc. MRM (2009) (Abstract 4788); [7] Virtual family models. Available at: http://www.itis.ethz.ch/index/index_humanmodels.html. [8] Cerqueira,MD, Circulation 2002; 105(4).539-42.